



Published in final edited form as:

J Proteome Res. 2012 April 6; 11(4): 2581–2593. doi:10.1021/pr300056m.

A C-Terminal Heat Shock Protein 90 Inhibitor Decreases Hyperglycemia-induced Oxidative Stress and Improves Mitochondrial Bioenergetics in Sensory Neurons

Liang Zhang[#], Huiping Zhao[^], Brian S.J. Blagg[^], and Rick T. Dobrowsky^{#,*}

[#]Department of Pharmacology and Toxicology, The University of Kansas, Lawrence, KS 66045

[^]Department of Medicinal Chemistry, The University of Kansas, Lawrence, KS 66045

Summary

Diabetic peripheral neuropathy (DPN) is a common complication of diabetes in which hyperglycemia-induced mitochondrial dysfunction and enhanced oxidative stress contribute to sensory neuron pathology. KU-32 is a novobiocin-based, C-terminal inhibitor of the molecular chaperone, heat shock protein 90 (Hsp90). KU-32 ameliorates multiple sensory deficits associated with the progression of DPN and protects unmyelinated sensory neurons from glucose-induced toxicity. Mechanistically, KU-32 increased the expression of Hsp70 and this protein was critical for drug efficacy in reversing DPN. However, it remained unclear if KU-32 had a broader effect on chaperone induction and if its efficacy was linked to improving mitochondrial dysfunction. Using cultures of hyperglycemicly stressed primary sensory neurons, the present study investigated whether KU-32 had an effect on the translational induction of other chaperones and improved mitochondrial oxidative stress and bioenergetics. A variation of stable isotope labeling with amino acids in cell culture called pulse SILAC (pSILAC) was used to unbiasedly assess changes in protein translation. Hyperglycemia decreased the translation of numerous mitochondrial proteins that affect superoxide levels and respiratory activity. Importantly, this correlated with a decrease in mitochondrial oxygen consumption and an increase in superoxide levels. KU-32 increased the translation of Mn superoxide dismutase and several cytosolic and mitochondrial chaperones. Consistent with these changes, KU-32 decreased mitochondrial superoxide levels and significantly enhanced respiratory activity. These data indicate that efficacy of modulating molecular chaperones in DPN may be due in part to improved neuronal mitochondrial bioenergetics and decreased oxidative stress.

Keywords

diabetes; hyperglycemia; SILAC; chaperones; sensory neurons; mitochondria; superoxide dismutase; oxidative stress

*Correspondence addressed to: Rick T. Dobrowsky, Department of Pharmacology and Toxicology, University of Kansas, 5064 Malott Hall, 1251 Wescoe Hall Dr., Lawrence, KS 66045, (785) 864-3531, fax-(785) 864-5219, dobrowsky@ku.edu.

Supporting Information Available: Supplemental Table 1 provides comprehensive information on the quantified and identified peptides and proteins. Column header information is provided in the first tab of the Excel file. The Quantified Proteins sheet provides information on proteins identified by at least two peptides that were used in the final analyses. The All Proteins sheet provides information on all proteins identified and quantified. The MsMs data sheet provides comprehensive information on the fragmentation of precursor peptides and assignment of fragment ions. This information is available free of charge via the Internet at <http://pubs.acs.org>.

Introduction

Diabetic peripheral neuropathy (DPN) is a neurodegenerative complication of diabetes that develops in 50–60% of diabetic patients¹. DPN has proven difficult to manage pharmacologically since it does not result from a single biochemical etiology that is manifested uniformly for the disease's duration (10 – 30 yrs). Molecular targets that are relatively “diabetes specific” (polyol & hexosamine pathways, advanced glycation end products) or which are altered in numerous disease states (PKC activation, altered neurotrophic support, enhanced oxidative stress) contribute to the progressive degeneration of small and large sensory fibers in DPN². However, current small molecule inhibitors of the above pathways/products have yielded few therapeutic agents. Clearly, the rational identification of new molecular paradigms that ameliorate DPN and offer “druggable” targets affords translational potential for improving the medical management of DPN.

Many neurodegenerative diseases fall into a class of protein-conformational disorders since their etiology is linked to the accumulation of specific mis-folded or aggregated proteins (for example, β -amyloid & tau in Alzheimer's disease)³. Though the etiology of DPN is not causally linked to the accrual of any one specific mis-folded or aggregated protein, hyperglycemia can increase oxidative stress⁴. The oxidative modification of amino acids^{5, 6} can impair protein folding³, decrease mitochondrial function and protein import^{2, 5, 7} and increase interaction with molecular chaperones⁸.

Molecular chaperones such as heat shock proteins 90 and 70 (Hsp90, Hsp70) are critical to folding nascent proteins. However, both of these chaperones are components of the cellular heat shock response (HSR). Numerous conditions that promote cell stress lead to the Hsp90-dependent induction of the HSR which, in part, promotes the transient up-regulation of Hsp70 to aid the refolding or clearance of aggregated and damaged proteins⁸. Hsp70 upregulation can also prevent neuronal apoptosis⁹ and decrease oxidative stress in neurodegenerative disorders¹⁰. Importantly, the HSR can be pharmacologically activated by inhibiting Hsp90 and we have developed and validated KU-32 as a novel, novobiocin-based, C-terminal Hsp90 inhibitor^{11, 12} that protects against *in vitro* neuronal cell death^{13, 14}. KU-32 also effectively reversed pre-existing psychosensory and electrophysiologic deficits of DPN in mice and its efficacy required Hsp70 as the drug was ineffective at reversing DPN modeled in Hsp70.1 and Hsp70.3 double knockout mice¹⁵. While these data clearly support that modulating molecular chaperones offers a potentially novel approach toward treating sensory neuron dysfunction in DPN, additional insight into the mechanism by which KU-32 may improve the function of glycemicly stressed neurons is needed.

Increased oxidative stress and mitochondrial dysfunction are strongly implicated in the pathogenesis of DPN^{5, 16}. Using variations of stable isotope labeling of amino acids in culture (SILAC), we have recently shown that numerous mitochondrial proteins are downregulated in response to hyperglycemia in cultured primary Schwann cells and dorsal root ganglia obtained from diabetic rats^{17, 18}. Importantly, decreases in the mitochondrial proteome correlated with a decrease in mitochondrial respiratory capacity¹⁸. However, as the level of all proteins is affected by the balance between their rates of synthesis versus degradation, these studies provided no insight into possible effects of hyperglycemia on the rate of protein translation. Indeed, little is known regarding the effect of hyperglycemia on rates of protein translation in sensory neurons.

In the present study, we took an unbiased approach to address the effect of hyperglycemia on protein translation using pulse SILAC (pSILAC)¹⁹. Moreover, since the mechanism of KU-32 invokes an increase in chaperone translation, we assessed the effect of hyperglycemia and KU-32 treatment on translation of mitochondrial proteins in sensory

neurons. We identify that hyperglycemia decreases the translation of numerous mitochondrial proteins and this correlates with an increase in mitochondrial superoxide levels and a decrease in mitochondrial respiratory function. KU-32 increased the overall rate of protein translation in glycemically stressed neurons, including several cytosolic and mitochondrial chaperones, components of the mitochondrial respiratory chain and Mn superoxide dismutase (MnSOD). Importantly, these changes correlated with a decrease in mitochondrial superoxide levels and increased mitochondrial respiratory capacity. Collectively, these data suggest that KU-32 may improve the sensory deficits associated with DPN by enhancing chaperone levels and improving mitochondrial function.

Experimental Procedures

Preparation of Embryonic Dorsal Root Ganglion Sensory Neurons

Dorsal root ganglion (DRG) neurons were dissected from embryonic day 15–18 rat pups and the ganglia were collected into L15 medium²⁰. The tissue was dissociated with 0.25% trypsin at 37°C for 30 min, the cells resuspended in DMEM containing 25 mM glucose, 10% fetal calf serum (FCS, Atlas Biologicals, Fort Collins, CO) and triturated with a firepolished glass pipette. The cells were counted and plated in the center of collagen coated (0.1 mg/mL collagen followed by overnight air drying in a laminar flow hood) 35 mm dishes at a density of $2-3 \times 10^5$ cells per dish. The cells were cultured in maintenance medium composed of DMEM (4.5 mg/ml glucose, 25 mM) containing 10% dialyzed FCS, 1× penicillin/streptomycin, 1X gentamicin and 50 ng/ml NGF (Harlan Biosciences, Indianapolis, IN). To remove proliferating cells, the neurons were treated with 10 μ M each of fluorodeoxyuridine and cytosine β -D-arabinoside for two days and the drugs withdrawn for 2 days; this cycle was repeated two more times. As the basal glucose concentration in the culture medium was 25 mM, hyperglycemia was induced by the addition of 20 mM excess glucose as we and others have described previously^{15, 21, 22}. All animal procedures were performed in accordance with protocols approved by the Institutional Animal Care and Use Committee and in compliance with standards and regulations for care and use of laboratory rodents set by the National Institutes of Health.

[³H]Leucine Pulse

To assess the global effect of hyperglycemia and KU-32 on protein translation, neurons were seeded in 12 well plates at 1×10^5 cells per well and treated for 5 days in the absence or presence of 20 mM excess glucose. During the final 24 hr of the incubation, the cells were treated with DMSO or 1 μ M KU-32 and pulsed with 1 μ Ci/ml L-[2,3,4,5-³H]Leucine (American Radiolabeled Chemicals, St. Louis MO). The cells were washed with ice-cold phosphate-buffered saline (PBS), scraped into 50 mM Tris-HCl, pH 7.4, 150 mM NaCl, 1 mM EDTA, 1% NP-40, 1× Complete[®] protease inhibitors (Roche Diagnostics, Indianapolis, IN) and an aliquot removed for protein determination. Equal amounts of total protein were precipitated by the addition of ice cold trichloroacetic acid to a final concentration of 25% and the precipitate was pelleted by centrifugation. The pellet was washed twice with -20°C acetone, air dried and radioactivity quantified by scintillation spectrometry.

pSILAC Labeling

Lysine (Lys)/Arginine (Arg) deficient DMEM and isotopically enriched (>98%) [²H₄] L-Lys; [¹³C₆] L-Arg; [¹³C₆, ¹⁵N₂] L-Lys and [¹³C₆, ¹⁵N₄] L-Arg were purchased from Sigma-Isotec (St. Louis, MO). For each neuron preparation, we performed three different sets of experiments to analyze the effect of hyperglycemia and KU-32 on protein translation. The isotopic mixtures and treatments used in the pSILAC¹⁹ experiments are summarized in Table 1. To assess the effect of hyperglycemia on translation, the neurons were cultured in maintenance medium containing 125 mg/l ¹²C-Lys and 84 mg/l ¹²C-Arg (KORO) in the

absence or presence of 20 mM excess glucose for 5 days. For the final 48 hrs of the incubation, control cultures were isotopically pulsed in DMEM supplemented with [$^2\text{H}_4$] Lys and [$^{13}\text{C}_6$] Arg (K4R6) while cells subjected to hyperglycemia were pulsed in culture medium containing [$^{13}\text{C}_6$, $^{15}\text{N}_2$]Lys and [$^{13}\text{C}_6$, $^{15}\text{N}_4$] Arg (K8R10). To assess the effect of KU-32 on translation under normoglycemic conditions, the drug was added for the final 24 hrs to neurons pulsed with K8R10; cells pulsed with K4R6 received DMSO. When assessing the effect of KU-32 on translation under hyperglycemic conditions, neurons were maintained in medium containing 20 mM excess glucose for 5 days and 1 μM KU-32 was added for the final 24 hrs to neurons pulsed with K4R6; DMSO was added to the cultures pulsed with K8R10. KU-32 [N-(7-((2R,3R,4S,5R)-3,4-dihydroxy-5-methoxy-6,6-dimethyl-tetrahydro-2H-pyran-2-yloxy)-8-methyl-2-oxo-2H-chromen-3-yl)acetamide] was synthesized and structural purity (>95%) verified as previously described²³.

At the end of the incubations, the cells were washed with ice-cold PBS and resuspended in 0.5 ml of mitochondrial isolation buffer (MIBA) containing 10 mM Tris-HCl, pH 7.4, 1 mM EDTA, 0.2 M D-mannitol, 0.05 M sucrose, 0.5 mM sodium orthovanadate, 1 mM sodium fluoride and 1 \times Complete[®] protease inhibitors²⁴. The cells were homogenized and the protein concentration of each lysate was measured in quadruplicate using the Bradford assay and bovine serum albumin as the standard. The samples were then mixed together in a 1:1 mass ratio and the combined lysate was centrifuged at $800 \times g$ for 10 min at 4°C. The supernatant was recovered, a heavy mitochondrial fraction isolated by centrifugation at $8,000 \times g$ for 5 min at 4°C and the pellet washed twice with ice-cold MIBA buffer. Three biological replicates were performed for the MS analysis using neurons obtained from separate litters of embryonic rat pups. Three additional biologic replicates using neurons obtained from separate litters were performed to validate some of the MS data using immunoblot analysis: monoclonal antibodies included Hsp70, mitochondrial Hsp70 and Hsc70 (Stressgen/Enzo Life Sciences, Farmingdale, NY); MnSOD (Upstate Biotechnology/Millipore, Billerica, MA) and β -actin (MP Biomedicals, Solon, OH). Hsp60 and Hsp70 protein 12A polyclonal and secondary antibodies were from Santa Cruz Biotechnology (Santa Cruz, CA).

Mass Spectrometry and Protein Identification

Proteins were identified following one-dimensional SDS-PAGE coupled to RP-HPLC linear quadrupole ion trap Fourier transform ion cyclotron resonance tandem mass spectrometry (GeLC-LTQ-FT MS/MS)²⁵. About 50 μg of protein was fractionated by SDS-PAGE, the proteins were visualized by staining the gel and the lanes were cut into 10–12 \times 0.5 cm sections for in-gel tryptic digestion.

Tryptic digestion of the proteins was performed as described previously^{17, 18}. The peptides were separated on a 0.30 \times 150 mm, Pepmap C₁₈ micro-capillary reverse-phase column at a flow rate of 5–10 $\mu\text{l}/\text{min}$ with a linear gradient from 5 to 65% acetonitrile in 0.06% aqueous formic acid (v/v) over 65 min. The eluate was introduced into the LTQ-FT tandem mass spectrometer (ThermoFinnigan, Waltham, MA) and mass spectra were acquired in the positive ion mode. All experiments were performed in data-dependent mode using dynamic exclusion with survey MS spectra (m/z 300–2000) acquired in the FT-ICR cell with resolution $R = 50,000$ at m/z 400 and accumulation to a target value of 5×10^5 charges, or a maximum ion accumulation time of 2000 ms. The five most intense ions were isolated and fragmented with a target value of 2×10^3 accumulated ions and an ion selection threshold of 3000 counts. Dynamic exclusion duration was typically 180 sec with early expiration if ion intensity fell below a S/N threshold of 2. The ESI source was operated with a spray voltage of 2.8 kV, a tube lens offset of 130 V and a capillary temperature of 200 °C. All other source parameters were optimized for maximum sensitivity of a synthetic YGGFL peptide ion at m/z 556.27.

Protein Identification and Quantification

Peak lists were acquired from the Xcalibur .raw files using MaxQuant v1.1.1.36²⁶. Protein identification utilized the integrated Andromeda search engine²⁷ queried against the rat IPI database (v3.80, 39,473 entries) that was concatenated with forward plus reverse sequences and supplemented with common contaminants. Search parameters specified a MS tolerance of 20 ppm, a fragment tolerance of 0.5 Da, up to 2 missed cleavages, 3 labeled amino acids per peptide and carboxyamidomethylated cysteine as a fixed modification. Variable modifications were set to consider methionine oxidation and protein N-terminal acetylation. It is not necessary to specify the isotopic labels as variable modifications when using the MaxQuant software²⁸ but the multiplicity was set to three to consider the K4R6 and K8R10 isotope combinations.

The experimental design template of MaxQuant was constructed such that the Xcalibur .raw MS files were grouped together for the three biological replicates (including any technical duplicates) for each treatment group shown in Table 1. For identification, peptides were required to be at least 6 amino acids in length and protein identification required at least one razor plus unique peptide. A protein was only included in the final analysis if it was identified by at least one peptide in two treatment groups. The false discovery rates were set to 1% at the peptide and protein levels. Posterior error probabilities (PEP, false hit probability given the peptide score and length)²⁶ ranged from 0 to 0.54 (95% of proteins had a PEP < 0.05) and after mass recalibration, the average absolute mass deviation was 1.62 ppm. Annotated MS/MS spectra were derived from the .raw files using the Viewer feature of MaxQuant.

For protein quantitation, we activated the requant feature and specified a single ratio count of unmodified and variably modified peptides for quantitation. For all the quantified peptides of a given protein, MaxQuant reports the median of these expression ratios and the non-normalized ratios are reported in Supplemental Table 1. Gene ontology (GO) annotations were obtained using the Uniprot identifier and the Perseus component of the MaxQuant software suite. Enrichment analyses were performed using the Database for Visualization and Integrated Discovery (DAVID)²⁹ and the Biological Networks Gene Ontology (BinGO)³⁰ plug-in of Cytoscape³¹.

Superoxide Assessment

Superoxide levels were measured by following the oxidation of dihydroethidine (Invitrogen-Molecular Probes, Carlsbad, CA) to ethidium³². Neurons were seeded at 1×10^4 cells per well in black 96 well plates and were treated with 25 mM or 45 mM glucose for five days. The cells received 1 μ M KU-32 or DMSO for the final 24 hrs of the incubation and the cells were subsequently treated with 15 μ M dihydroethidine for 15 mins at 37°C. After washing with PBS, the ratio of ethidium (excitation 530 nm, emission 590 nm) to dihydroethidine (excitation 485 nm, emission 530 nm) was determined using a fluorescence spectrometer.

To directly assess mitochondrial superoxide production, the cells were treated as above and washed once with phenol free Neurobasal medium. MitoTracker Green (80 nM) and 0.4 μ M MitoSOX Red were added to each well and incubated for 10 min³³. The cells were washed twice with fresh Neurobasal medium prior to imaging on an Olympus 3I Spinning Disk confocal microscope using excitation/emission wavelengths of 575/624 nm (MitoSox Red) and 494/531 nm (MitoTracker Green)³⁴. As a positive control, some cells were treated with 1.8 μ g/ml antimycin A for 25 mins. Fluorescence intensity of the red and green signals of at least 200 cells per treatment was obtained using CellProfiler and CellProfiler Analyst image analysis software.

Mitochondrial Respiration

O₂ consumption rate (OCR) was assessed using intact DRG sensory neurons and a XF96 Extracellular Flux Analyzer (Seahorse Biosciences, North Billerica, MA). Extracellular flux analysis is a non-invasive assay which uses two calibrated optical sensors to directly measure OCR in real-time in neurons that remain attached to the culture plate³⁵. Primary embryonic sensory neurons were seeded in the 96 well plates at 1.5×10^4 cells per well and treated for 5 days in 25 mM or 45 mM glucose. Cells were treated with 1 μ M KU-32 or DMSO for the final 24 hr of the incubation and the cells were placed in fresh bicarbonate-free DMEM containing 5 mM glucose and 1 mM pyruvate. Baseline OCR was assessed in the XF96 analyzer using 4 measurement loops consisting of a 2 minute mix cycle and a 5 min measurement cycle. Respiratory chain inhibitors were then sequentially injected into the wells and ATP-coupled oxygen consumption was calculated as the fraction of the basal OCR sensitive to 1 μ g/ml oligomycin, an ATP synthase inhibitor. The maximal uncoupled respiration rate was determined by depolarizing the mitochondrial membrane potential with 1 μ M FCCP (carbonylcyanide-4-(trifluoromethoxy)-phenylhydrazone). The cell seeding density and inhibitor concentrations were optimized in preliminary experiments. After the respiratory measures, the cells were harvested and experimental rate values were normalized to protein content of each well. Maximal respiratory capacity, spare respiratory capacity and respiratory state apparent (State_{app}) were determined from the rate data as described^{36, 37}.

Statistical Analyses

All statistical differences between treatments were determined using ProStat (v4.83). Data were analyzed using either a one-way ANOVA and Tukey's post hoc test or a Kruskal-Wallis test and Dunn's post-hoc analysis.

Results and Discussion

We have shown previously that 2–3 week old cultures of embryonic sensory neurons can serve as a cell model to examine mechanisms of hyperglycemic stress^{15, 21}. After two weeks in culture, embryonic sensory neurons were subjected to five days of hyperglycemia and the global effect on protein translation was measured by pulsing the cells with [³H]Leu for the final 24 hrs. Hyperglycemic-stressed neurons showed a 22% decrease in [³H]Leu incorporation and treating the cells with 1 μ M KU-32 for 24 hr prior to the Leu pulse significantly increased overall translation (Fig. 1). These results suggest that modulating chaperones may broadly increase protein translation.

To identify specific proteins whose translation was differentially effected by hyperglycemia and KU-32, we utilized the pSILAC strategy that has been previously described¹⁹ and is outlined in Fig. 2. To assess the effect of KU-32 on protein translation in hyperglycemic stressed sensory neurons, neurons were incubated in KOR0 culture medium containing 45 mM glucose. After 3 days, the KOR0 cultures were divided such that one set of cells was placed in hyperglycemic culture medium containing medium-heavy forms of Lys and Arg (K4R6). The cells were pulsed with K4R6 for 48 hrs and treated with 1 μ M KU-32 for the final 24 hr of the incubation. The remaining KOR0 cells were placed in hyperglycemic culture medium containing heavy isotope forms of Lys and Arg (K8R10) and treated with DMSO for the final 24 hr of the incubation. During the isotopic pulse, all newly synthesized proteins can only incorporate the K4R6 or K8R10 forms of Lys and Arg. Total cell lysates were prepared from the two treatment groups and mixed in a 1:1 mass ratio prior to isolation of subcellular fractions. Following mass spectrometric analysis, the abundance ratio of a K4/K8 or R6/R10 peptide reflects the difference in translation of the associated protein due to KU-32 treatment under hyperglycemic conditions (Table 1). Since all the KOR0 peptides

associated with a given protein are present prior to the pulse, they can be ignored as they do not represent newly translated protein¹⁹.

MaxQuant identified 743 proteins, of which 577 were identified by at least 2 peptides and 280 were quantified (Supplementary Table 1). Approximately one-third of the 280 quantified proteins were present in all of the treatments (Fig. 3A) and of the 156 proteins annotated as mitochondrial, 79 were quantified. Though the log 2 distributions of the protein expression ratios for each treatment were relatively unimodal, they were asymmetric and consistent with hyperglycemia decreasing protein translation and KU-32 treatment of hyperglycemic cells increasing translation (Fig. 3B). To determine what biological processes may be over-represented following KU-32 treatment, proteins showing at least a 1.5 fold increase were submitted to enrichment analysis using DAVID and the BinGO plug-in of Cytoscape. Both analyses supported that protein folding and response to reactive oxygen species were among the enriched biological processes identified (both ~ 11 fold enrichment).

KU-32 Effects Expression of Multiple Molecular Chaperones

The effect of hyperglycemia in absence and presence of KU-32 treatment on the expression of chaperones (green) and proteins with a mitochondrial annotation (red) is shown in Fig. 3C. We have shown previously that KU-32 induces cytosolic Hsp70¹³ and rather unexpectedly, we did not detect this Hsp70 paralog in any treatment group. This may be due to its relatively low abundance in the neurons compared to the constitutive form of Hsp70 (Hsc70), which is highly abundant and has a similar molecular weight (Fig. 3D). Although an enriched mitochondrial preparation was used in the analysis, cytosolic Hsc70 was among the top ten identifications based on total number of peptides identified, but was not significantly modified in any treatment. However, immunoblot analysis of whole cell lysates revealed that KU-32 significantly increased Hsp70 expression in hyperglycemic stressed neurons (Fig. 3D).

A surprising finding of the pSILAC analysis was that KU-32 also increased mitochondrial chaperones under hyperglycemic conditions. Hsp60 is necessary to ensure the proper folding of proteins imported into the mitochondrial matrix³⁸ and compared to hyperglycemia alone, KU-32 promoted a median increase in translation of 3.7-fold (Fig 3C). An example of a pSILAC isotopic triplet of mtHsp60 is shown in Fig. 4A. As expected, the unlabeled AAVEGIVIGGGCAII(R0) peptide is of substantially greater intensity than the newly translated labeled peptides (note 5X scale amplification for the K4R6 and K8R10 peaks) since it existed prior to the pulse and its intensity has additive contributions from sample mixing. When comparing the R6 and R10 forms of the peptide as indicative of newly translated protein, KU-32 treatment (R6 peptide at m/z 845.97) clearly enhanced the translation of Hsp60 relative to hyperglycemia alone (note that the mass differences between the peaks are one-half the expected amu shift since the peptides are doubly charged). In contrast, Hsp10 is a mitochondrial chaperone that was identified but not quantified in any treatment, suggesting that it had a lower rate of translation.

Mortalin/Grp75/stress-70 protein is a mitochondrial Hsp70 (mtHsp70) family member that is a component of the presequence translocase-associated motor complex³⁹ and its translation was modestly decreased by hyperglycemia. Similar to Hsp60, the identification of mtHsp70 was by numerous peptides in each treatment. Fig. 4B shows the MS/MS spectra of a peptide that was identified by seven sequential y- and b-ions that KU-32 increased about 1.8-fold in cells subjected to hyperglycemic stress (Fig. 4C). Importantly, immunoblot analysis from 3 separate neuronal cultures further verified this finding (Fig. 4C). In contrast to Hsp60, mtHsp70 is not induced as part of the classic heat shock response, however, it is upregulated in response to other forms of cell stress and its over-expression can improve

mitochondrial function during focal ischemia⁴⁰. Additionally, about 99% of mitochondrial proteins are nuclear encoded and require translocation and import into the organelle³⁹. Although little is known on the effect of diabetes on mitochondrial protein import in sensory neurons, diabetes decreased the rate of protein import into interfibrillar, but not subsarcolemmal cardiac mitochondria⁷. Since mtHsp70 and Hsp60 are respectively involved in the import and folding of proteins into the mitochondrial matrix³⁸, these data suggest that KU-32 may affect mitochondrial function by facilitating protein import and maturation.

KU-32 also promoted a 4.9-fold increase in the expression of another Hsp70 paralog, Hsp70 protein 12A (Hsp70 p12A), and this was verified by immunoblot analysis of separate neuronal cultures (Fig. 4D). Hsp70 p12A is an atypical member of the Hsp70 family and despite the fact that *HSPA12* genes evolved early in the evolution of vertebrates⁴¹, the protein's localization and function remain poorly characterized. Recent reports have provided descriptions that Hsp70 p12A expression is decreased in pre-frontal cortex of schizophrenic brain⁴² and increased in arteriosclerotic lesions⁴³, but no functional properties were ascribed to these observations. Since Hsp70 p12A contains atypical ATPase and substrate binding domains⁴¹, it may function as a co-chaperone.

Neither Hsp90 α nor Hsp90 β were significantly altered by KU-32 in the hyperglycemic neurons. Curiously, KU-32 induced a 1.5-fold increase in calnexin translation, which is a chaperone involved in protein quality control in the endoplasmic reticulum (ER). However, other ER chaperones such as Grp78 and Grp94 were readily identified by numerous peptides but not quantified, suggesting that they were not undergoing substantial changes in translation. Together, these data support that in hyperglycemic stressed neurons, inhibiting the C-terminus of Hsp90 is sufficient to increase several Hsp70 family members and other mitochondrial chaperones.

KU-32 Increased MnSOD Translation and Decreased Glucose-induced Superoxide Production

An established hallmark of mitochondrial dysfunction in DPN is the induction of oxidative stress, due in part to an increase in mitochondrial superoxide production⁴. Consistent with these data and our previous results¹⁸, translation of MnSOD in hyperglycemic stressed neurons was about 50% less than that measured in control neurons (3 peptides quantified) and KU-32 promoted a 2.3 fold increase in the translation of MnSOD (Fig. 5A) in the hyperglycemic stressed cells. Although only quantified by 2 peptides, the identification of this doubly charged peptide was substantiated by a sequential series of 10 b-ions and 11 y-ions (Fig. 5B). Moreover, immunoblot analysis of separate neuronal cultures verified that hyperglycemia decreased MnSOD and that KU-32 treatment significantly increased its expression (Fig. 5A).

To determine if the increase in MnSOD by KU-32 corresponded to a decrease in superoxide production, the ratio of ethidium/dihydroethidium was used as a non-organelle selective measure of superoxide. Neurons were pre-treated with vehicle or KU-32 and exposed to 45 mM glucose for 6 hrs to acutely increase superoxide levels²². Hyperglycemia increased superoxide levels and KU-32 significantly blocked this effect (Fig. 5C). To determine if KU-32 prevented superoxide production within mitochondria in neurons subjected to the more chronic hyperglycemic stress that was used in the proteomic analyses, we used MitoSox red and the mitochondrial marker, MitoTracker Green. Five days of hyperglycemia increased mitochondrial superoxide levels and treating the cells with KU-32 for the final 24 hrs significantly decreased this response (Figs. 5D & 5E). As a positive control, some neurons were treated with antimycin A prior to the addition of the dyes. These data support that modulating the activity of Hsp90 with KU-32 is sufficient to increase MnSOD and decrease glucose-induced mitochondrial oxidative stress.

Increased Translation of Mitochondrial Chaperones and MnSOD by KU-32 Correlates with an Improved Bioenergetic Profile

Hyperglycemia-induced oxidative stress renders mitochondrial proteins more susceptible to oxidative damage. Relative to their rate of production, a slower rate of repair by mitochondrial chaperones favors accumulation of oxidatively damaged proteins in the organelle⁴⁴. Thus, the ability of KU-32 to increase mitochondrial chaperones and decrease oxidative stress suggests that the bioenergetic profile of the organelle may also be enhanced. To this end, we used a XF96 Extracellular Flux Analyzer to assess the effect of hyperglycemia and KU-32 treatment on oxygen consumption rate (OCR). The XF96 analyzer measures OCR in real time using intact cells and results in Fig. 6A show a typical mitochondrial function experiment from ~5,000 sensory neurons per well (n=4) respiring in DMEM containing 5.5 mM glucose. The first four rates represent basal OCR (light blue shading) and each rate measure was normalized to the total amount of protein per well and expressed as a percent of the final basal OCR (rate 4). Measuring OCR in intact cells in the absence and presence of respiratory chain poisons is the single most useful test to stringently assess mitochondrial dysfunction³⁶. Oligomycin is an ATP synthase inhibitor and its injection decreases the basal OCR. The magnitude of this decrease is indicative of the percent of the basal OCR that is coupled to ATP synthesis (dark blue shading) and the residual OCR is due to proton leak (uncoupled respiration). FCCP is a protonophore whose addition provides a measure of maximal respiratory capacity (MRC, red shading). MRC assesses the functional integrity of the respiratory chain since electron transfer is no longer rate limited by the proton gradient across the inner mitochondrial membrane³⁶. Nicholls has defined spare respiratory capacity (SRC) as the arithmetic difference between MRC and the basal OCR (pink shading)⁴⁵. SRC provides a functional indication of how close to its bioenergetic limit a cell is respiring³⁶. A loss of SRC, especially in neurons that have variable ATP demands, limits their ability to match energetic needs to environmental demands and renders the cells more susceptible to secondary stressors^{46, 47}. Thus, treatment-induced differences in MRC and SRC are indicative of mitochondrial dysfunction affecting the bioenergetic limits and reserve capacity of the neurons. Although not measured in the current experiment, the green shading is representative of non-mitochondrial OCR values obtained the presence of rotenone and antimycin A to inhibit complexes I and III, respectively.

Neurons were incubated in medium containing 25 or 45 mM glucose for 5 days and treated with KU-32 for the final 24 hrs. To assess respiration under a standard glucose concentration, the cells were placed in serum-free DMEM containing 5.5 mM glucose and 1 mM pyruvate at 37°C for 1 hr prior to measuring OCR. After measuring basal OCR, the cells were exposed to oligomycin and no significant differences were observed in the magnitude of ATP-coupled OCR and proton leak (Fig. 6B). In contrast, though FCCP stimulated MRC above basal OCR in all treatments, neurons exposed to hyperglycemic stress exhibited a significantly blunted MRC relative to control cells (Fig. 6B). Similarly, SRC was also significantly decreased in the glycemically stressed cells compared to control (Fig. 6C, solid bars).

In cells maintained in 25 mM glucose and treated with KU-32, the average MRC and SRC was slightly decreased but this was not significantly different from control. Consistent with the efficacy of KU-32 in decreasing mitochondrial superoxide levels, glycemically stressed cells treated with the drug showed a significant improvement in both MRC (Fig. 6B) and SRC (Fig. 6C, solid bars) compared to the neurons incubated in high glucose alone. The blunted MRC and SRC apparent in the hyperglycemically stressed cells supports that they are energetically stressed and that mitochondrial workload is increased.

The respiratory state apparent ($State_{app}$) provides a quantitative indication of mitochondrial workload and can be estimated from these data⁴⁷. As mitochondrial workload decreases, $State_{app}$ approaches 4, a metabolic indicator that minimal ATP-coupled respiration is needed and OCR is primarily uncoupled⁴⁷. On the other hand, high ATP demand requires state 3.0 respiration (comparable to that induced by FCCP, Fig. 6B). The $State_{app}$ values were 3.5 ± 0.5 and 3.5 ± 0.3 in neurons treated with vehicle or KU-32, respectively, indicating the basal mitochondrial workload required to meet ATP needs. In contrast, hyperglycemia promoted a significant decrease in $State_{app}$ (3.3 ± 0.3 , Fig. 6C, striped bars), suggesting that ATP demand is depleting reserve capacity and that the organelles are approaching bioenergetic failure³⁷. Importantly, KU-32 treatment significantly improved this decline. The ability of KU-32 to increase MRC, SRC and $State_{app}$ supports that the cells have recovered significant respiratory capacity that correlates with the induction of mitochondrial chaperones and a decrease in superoxide production. Although numerous factors contribute to OCR³⁷, hyperglycemia-induced damage to respiratory chain proteins may decrease the efficiency of electron transport to affect SRC and increase mitochondrial workload.

Conclusions

Our previous work on novobiocin-based C-terminal Hsp90 inhibitors has demonstrated that they induce Hsp70 and protect cortical and sensory neurons from toxicity induced by β -amyloid peptides and hyperglycemia, respectively^{13, 15}. Although the neuroprotective efficacy of KU-32 in reversing DPN required the presence of Hsp70, the current study sought to unbiasedly identify whether KU-32 promoted the translation of other proteins that may aid sensory neurons in tolerating glucotoxic stress⁴⁸. Using pSILAC, we identify that mitochondrial chaperones and MnSOD are also increased by KU-32 treatment of hyperglycemic cells. Consistent with the induction of MnSOD, KU-32 decreased mitochondrial superoxide levels in neurons subjected to 5 days of hyperglycemia. Similarly, hyperglycemia decreased various measures of mitochondrial respiratory capacity and treating the neurons with KU-32 significantly improved both maximum and spare respiratory capacity.

Previous investigators have shown that embryonic sensory neurons cultured in vitro for 3 days are susceptible to glucose-induced apoptosis^{49, 50}. However, 2–3 week old cultures of embryonic sensory neurons are resistant to glucose-induced cell death^{11, 17}, similar to adult sensory neurons⁵¹. Although the more differentiated embryonic neurons can serve as a cell model to examine mechanisms of hyperglycemic stress unrelated to apoptosis, their response to hyperglycemia does not necessarily mimic that observed in adult neurons. For example, hyperglycemia induced a robust increase in superoxide in adult sensory neurons isolated from chronically diabetic mice but not from neurons obtained from control animals^{18, 52}. Thus, obtaining sensory neurons from adult diabetic animals that have received drug treatment will also be a beneficial approach toward dissecting the mechanism of drug efficacy on improving mitochondrial function. Although correlative, since mitochondrial function is clearly compromised in DPN^{18, 52, 53}, the improved expression of mitochondrial chaperones and enhanced respiratory capacity may at least partially underlie the efficacy of KU-32 in reversing sensory hypoalgesia in diabetic mice¹⁵. We would like to emphasize that our approach in using the differentiated embryonic neurons has no implications on the role or relevance of glucose-induced apoptosis to DPN. The neuroprotective properties of KU-32 in ameliorating DPN are unlikely to center on preventing sensory neuron death since apoptosis has not been demonstrated as a key feature in the development of DPN^{54, 55, 56}.

It is important to note that Hsp70 is a necessary component of drug efficacy since gene deletion of inducible forms of Hsp70 ablated the ability of KU-32 therapy to reverse several

indices of experimental DPN¹¹. However, this does not rule out that the induction of mitochondrial chaperones and MnSOD are not a critical aspect of the effect of KU-32 on improving mitochondrial function, and by extension, DPN. Emerging data supports that diabetes increases oxidative stress and mitochondrial fission/fusion in sensory neurons⁵⁷⁻⁵⁹. Decreasing oxidative stress and maintaining the fidelity of protein import to support this turnover would be essential to maximizing the bioenergetic capacity of the organelle. As both Hsp70 and mtHsp70 aid mitochondrial protein import via separate import pathways³⁹, we hypothesize that these proteins may enhance mitochondrial bioenergetics by facilitating the import of respiratory and anti-oxidant proteins; MnSOD is imported into the mitochondrial matrix via mtHsp70. To this end, it will be critical to define whether the necessity of Hsp70 induction for drug efficacy is related to improved mitochondrial function and/or protein import. Similarly, the sufficiency/necessity of mtHsp70 and MnSOD induction by KU-32 to improving mitochondrial function in response to hyperglycemic stress remains to be determined.

In conclusion, the salient findings of this study provide proof-of-principle that a novel C-terminal Hsp90 inhibitor can decrease mitochondrial superoxide levels and improve organellar bioenergetics in hyperglycemic stressed neurons. These functional improvements correlated with the translational induction of MnSOD and mitochondrial chaperones by KU-32. Thus, the reported efficacy of KU-32 therapy in ameliorating sensory hypoalgesia in DPN may relate to improved mitochondrial function.

Supplementary Material

Refer to Web version on PubMed Central for supplementary material.

Acknowledgments

This work was supported by grants from the Juvenile Diabetes Research Foundation (RTD) and The National Institutes of Health (NS054847, DK073594 to RTD) and (CA120458, CA109265 to BSJB).

Abbreviations

BinGO	Biological Networks Gene Ontology
dFCS	dialyzed fetal calf serum
DPN	diabetic peripheral neuropathy
GeLC-LTQ-FT MS/MS	gel electrophoresis and liquid chromatography linear quadrupole ion trap Fourier transform ion cyclotron resonance tandem mass spectrometry
GO	Gene Ontology
Hsp	heat shock protein
MnSOD	manganese superoxide dismutase
OCR	oxygen consumption rate
PBS	phosphate buffered saline
pSILAC	pulse stable-isotope labeling with amino acids in cell culture

References

1. Calcutt NA, Cooper ME, Kern TS, Schmidt AM. Therapies for hyperglycaemia-induced diabetic complications: From animal models to clinical trials. *Nat Rev Drug Discov.* 2009; 8:417–430. [PubMed: 19404313]
2. Tomlinson DR, Gardiner NJ. Glucose neurotoxicity. *Nat Rev Neurosci.* 2008; 9:36–45. [PubMed: 18094705]
3. Muchowski PJ, Wacker JL. Modulation of neurodegeneration by molecular chaperones. *Nat Rev Neurosci.* 2005; 6:11–22. [PubMed: 15611723]
4. Pop-Busui R, Sima A, Stevens M. Diabetic neuropathy and oxidative stress. *Diabetes Metab. Res. Rev.* 2006; 22:257–273. [PubMed: 16506271]
5. Obrosova IG. Diabetes and the peripheral nerve. *Biochim Biophys Acta.* 2009; 10:931–940. [PubMed: 19061951]
6. Akude E, Zherebitskaya E, Roy Chowdhury SK, Girling K, Fernyhough P. 4-hydroxy-2-nonenal induces mitochondrial dysfunction and aberrant axonal outgrowth in adult sensory neurons that mimics features of diabetic neuropathy. *Neurotox Res.* 2009; 1:28–38. [PubMed: 19557324]
7. Baseler WA, Dabkowski ER, Williamson CL, Croston TL, Thapa D, Powell MJ, Razunguzwa TT, Hollander JM. Proteomic alterations of distinct mitochondrial subpopulations in the type 1 diabetic heart: Contribution of protein import dysfunction. *Am J Physiol Regul Integr Comp Physiol.* 2011; 300:R186–R200. [PubMed: 21048079]
8. Pratt WB, Morishima Y, Peng HM, Osawa Y. Proposal for a role of the hsp90/hsp70-based chaperone machinery in making triage decisions when proteins undergo oxidative and toxic damage. *Exp Biol Med.* 2010; 235:278–289.
9. Bienemann AS, Lee YB, Howarth J, Uney JB. Hsp70 suppresses apoptosis in sympathetic neurones by preventing the activation of c-jun. *J Neurochem.* 2008; 104:271–278. [PubMed: 17971127]
10. Chaudhury S, Welch TR, Blagg BS. Hsp90 as a target for drug development. *Chem Med Chem.* 2006; 1:1331–1340. [PubMed: 17066389]
11. Matts RL, Brandt GE, Lu Y, Dixit A, Mollapour M, Wang S, Donnelly AC, Neckers L, Verkhivker G, Blagg BS. A systematic protocol for the characterization of hsp90 modulators. *Bioorg Med Chem.* 2011; 19:684–692. [PubMed: 21129982]
12. Matts RL, Dixit A, Peterson LB, Sun L, Voruganti S, Kalyanaraman P, Hartson SD, Verkhivker GM, Blagg BS. Elucidation of the hsp90 c-terminal inhibitor binding site. *ACS Chem Biol.* 2011
13. Ansar S, Burlison JA, Hadden MK, Yu XM, Desino KE, Bean J, Neckers L, Audus KL, Michaelis ML, Blagg BS. A non-toxic hsp90 inhibitor protects neurons from abeta-induced toxicity. *Bioorg Med Chem Lett.* 2007; 17:1984–1990. [PubMed: 17276679]
14. Lu Y, Ansar S, Michaelis ML, Blagg BS. Neuroprotective activity and evaluation of hsp90 inhibitors in an immortalized neuronal cell line. *Bioorg Med Chem.* 2008; 17:1709–1715. [PubMed: 19138859]
15. Urban MJ, Li C, Yu C, Lu Y, Krise JM, McIntosh MP, Rajewski RA, Blagg BSJ, Dobrowsky RT. Inhibiting heat shock protein 90 reverses sensory hypoalgesia in diabetic mice. *ASN Neuro.* 2010; 2:189–199. e00040 DOI.
16. Chowdhury SKR, Dobrowsky RT, Fernyhough P. Nutrient excess and altered mitochondrial proteome and function contribute to neurodegeneration in diabetes. *Mitochondrion.* 2011; 11:845–854. [PubMed: 21742060]
17. Zhang L, Yu C, Vasquez FE, Galeva N, Onyango I, Swerdlow RH, Dobrowsky RT. Hyperglycemia alters the schwann cell mitochondrial proteome and decreases coupled respiration in the absence of superoxide production. *J Proteome Res.* 2010; 9:458–471. [PubMed: 19905032]
18. Akude E, Zherebitskaya E, Chowdhury SKR, Smith DR, Dobrowsky RT, Fernyhough P. Diminished superoxide generation is associated with respiratory chain dysfunction and changes in the mitochondrial proteome of sensory neurons from diabetic rats. *Diabetes.* 2011; 60:288–297. [PubMed: 20876714]
19. Schwanhauser B, Gossen M, Dittmar G, Selbach M. Global analysis of cellular protein translation by pulsed silac. *Proteomics.* 2009; 9:205–209. [PubMed: 19053139]

20. Zanazzi G, Einheber S, Westreich R, Hannocks MJ, Bedell-Hogan D, Marchionni MA, Salzer JL. Glial growth factor/neuregulin inhibits schwann cell myelination and induces demyelination. *J. Cell Biol.* 2001; 152:1289–1299. [PubMed: 11257128]
21. Yu C, Rouen S, Dobrowsky RT. Hyperglycemia and downregulation of caveolin-1 enhance neuregulin-induced demyelination. *Glia.* 2008; 56:877–887. [PubMed: 18338795]
22. Vincent AM, Kato K, McLean LL, Soules ME, Feldman EL. Sensory neurons and schwann cells respond to oxidative stress by increasing antioxidant defense mechanisms. *Antioxid Redox Signal.* 2009; 11:425–438. [PubMed: 19072199]
23. Huang Y-T, Blagg BSJ. A library of noviosylated coumarin analogues. *J. Org. Chem.* 2007; 72:3609–3613. [PubMed: 17328573]
24. Okado-Matsumoto A, Fridovich I. Subcellular distribution of superoxide dismutases (sod) in rat liver. Cu,zn-sod in mitochondria. *J. Biol. Chem.* 2001; 276:38388–38393. [PubMed: 11507097]
25. Steen H, Mann M. The abc's (and xyz's) of peptide sequencing. *Nat. Rev Mol Cell Biol.* 2004; 5:699–711. [PubMed: 15340378]
26. Cox J, Mann M. Maxquant enables high peptide identification rates, individualized p.P.B.-range mass accuracies and proteome-wide protein quantification. *Nat Biotechnol.* 2008; 26:1367–1372. [PubMed: 19029910]
27. Cox, Jr; Neuhauser, N.; Michalski, A.; Scheltema, RA.; Olsen, JV.; Mann, M. Andromeda: A peptide search engine integrated into the maxquant environment. *J. Proteome Res.* 2011; 10:1794–1805. [PubMed: 21254760]
28. Cox J, Matic I, Hilger M, Nagaraj N, Selbach M, Olsen JV, Mann M. A practical guide to the maxquant computational platform for silac-based quantitative proteomics. *Nat Protoc.* 2009; 4:698–705. [PubMed: 19373234]
29. Huang DW, Sherman BT, Lempicki RA. Systematic and integrative analysis of large gene lists using david bioinformatics resources. *Nat. Protocols.* 2008; 4:44–57.
30. Maere S, Heymans K, Kuiper M. Bingo: A cytoscape plugin to assess overrepresentation of gene ontology categories in biological networks. *Bioinformatics.* 2005; 21:3448–3449. [PubMed: 15972284]
31. Shannon P, Markiel A, Ozier O, Baliga NS, Wang JT, Ramage D, Amin N, Schwikowski B, Ideker T. Cytoscape: A software environment for integrated models of biomolecular interaction networks. *Genome Res.* 2003; 13:2498–2504. [PubMed: 14597658]
32. Vincent AM, McLean LL, Backus C, Feldman EL. Short-term hyperglycemia produces oxidative damage and apoptosis in neurons. *FASEB J.* 2005; 19:638–640. [PubMed: 15677696]
33. Robinson KM, Janes MS, Beckman JS. The selective detection of mitochondrial superoxide by live cell imaging. *Nat Protoc.* 2008; 3:941–947. [PubMed: 18536642]
34. Mukhopadhyay P, Rajesh M, Hasko G, Hawkins BJ, Madesh M, Pacher P. Simultaneous detection of apoptosis and mitochondrial superoxide production in live cells by flow cytometry and confocal microscopy. *Nat Protoc.* 2007; 2:2295–2301. [PubMed: 17853886]
35. Wu M, Neilson A, Swift AL, Moran R, Tamagnine J, Parslow D, Armistead S, Lemire K, Orrell J, Teich J, Chomicz S, Ferrick DA. Multiparameter metabolic analysis reveals a close link between attenuated mitochondrial bioenergetic function and enhanced glycolysis dependency in human tumor cells. *Am J Physiol Cell Physiol.* 2007; 292:C125–C136. [PubMed: 16971499]
36. Brand MD, Nicholls DG. Assessing mitochondrial dysfunction in cells. *Biochem J.* 2011; 435:297–312. [PubMed: 21726199]
37. Sansbury BE, Jones SP, Riggs DW, Darley-Usmar VM, Hill BG. Bioenergetic function in cardiovascular cells: The importance of the reserve capacity and its biological regulation. *Chemico-Biolog Interact.* 2011; 191:288–295.
38. Deocaris CC, Kaul SC, Wadhwa R. On the brotherhood of the mitochondrial chaperones mortalin and heat shock protein 60. *Cell Stress Chaperones.* 2006; 11:116–128. [PubMed: 16817317]
39. Schmidt O, Pfanner N, Meisinger C. Mitochondrial protein import: From proteomics to functional mechanisms. *Nat Rev Mol Cell Biol.* 2010; 11:655–667. [PubMed: 20729931]
40. Xu L, Voloboueva LA, Ouyang Y, Emery JF, Giffard RG, Yang H, Zhou X, Liu X, Yang L, Chen Q, Zhao D, Zuo J, Liu W. Overexpression of mitochondrial hsp70/hsp75 in rat brain protects mitochondria, reduces oxidative stress, and protects from focal ischemia mitochondrial

dysfunction induced by knockdown of mortalin is rescued by parkin. *J. Cerebral Blood Flow Metab.* 2009; 29:365–374.

41. Brocchieri L, Conway de Macario E, Macario AJ. Hsp70 genes in the human genome: Conservation and differentiation patterns predict a wide array of overlapping and specialized functions. *BMC Evol Biol.* 2008; 8:19. [PubMed: 18215318]
42. Pongrac JL, Middleton FA, Peng L, Lewis DA, Levitt P, Mirmics K. Heat shock protein 12a shows reduced expression in the prefrontal cortex of subjects with schizophrenia. *Biol Psychiatry.* 2004; 56:943–950. [PubMed: 15601604]
43. Han Z, Truong QA, Park S, Breslow JL. Two hsp70 family members expressed in atherosclerotic lesions. *Proc Natl Acad Sci U S A.* 2003; 100:1256–1261. [PubMed: 12552099]
44. Deocaris C, Kaul S, Wadhwa R. From proliferative to neurological role of an hsp70 stress chaperone, mortalin. *Biogerontology.* 2008; 9:391–403. [PubMed: 18770009]
45. Nicholls DG, Johnson-Cadwell L, Vesce S, Jekabsons M, Yadava N. Bioenergetics of mitochondria in cultured neurons and their role in glutamate excitotoxicity. *J Neurosci Res.* 2007; 85:3206–3212. [PubMed: 17455297]
46. Choi SW, Gerencser AA, Nicholls DG. Bioenergetic analysis of isolated cerebrocortical nerve terminalson a microgram scale: Spare respiratory capacity and stochastic mitochondrial failure. *J. Neurochem.* 2009; 109:1179–1191. [PubMed: 19519782]
47. Dranka BP, Hill BG, Darley-Usmar VM. Mitochondrial reserve capacity in endothelial cells: The impact of nitric oxide and reactive oxygen species. *Free Rad Biol Med.* 2010; 48:905–914. [PubMed: 20093177]
48. Calcutt NA. Tolerating diabetes - an alternative therapeutic approach for diabetic neuropathy. *ASN Neuro.* 2010; 2:215–217.
49. Russell JW, Sullivan KA, Windebank AJ, Herrmann DN, Feldman EL. Neurons undergo apoptosis in animal and cell culture models of diabetes. *Neurobiol. Dis.* 1999; 6:347–363. [PubMed: 10527803]
50. Russell JW, Golovoy D, Vincent AM, Mahendru P, Olzmann JA, Mentzer A, Feldman EL. High glucose-induced oxidative stress and mitochondrial dysfunction in neurons. *FASEB J.* 2002; 16:1738–1748. [PubMed: 12409316]
51. Fernyhough P, Roy Chowdhury SK, Schmidt RE. Mitochondrial stress and the pathogenesis of diabetic neuropathy. *Expert Rev Endocrinol Metab.* 2010; 5:39–49. [PubMed: 20729997]
52. Zherebitskaya E, Akude E, Smith DR, Fernyhough P. Development of selective axonopathy in adult sensory neurons isolated from diabetic rats: Role of glucose-induced oxidative stress. *Diabetes.* 2009; 58:1356–1364. [PubMed: 19252136]
53. Chowdhury SK, Zherebitskaya E, Smith DR, Akude E, Chattopadhyay S, Jolivald CG, Calcutt NA, Fernyhough P. Mitochondrial respiratory chain dysfunction in dorsal root ganglia of streptozotocin-induced diabetic rats and its correction by insulin treatment. *Diabetes.* 2010; 59:1082–1091. [PubMed: 20103706]
54. Kishi M, Tanabe J, Schmelzer JD, Low PA. Morphometry of dorsal root ganglion in chronic experimental diabetic neuropathy. *Diabetes.* 2002; 51:819–824. [PubMed: 11872686]
55. Zochodne DW, Verge VMK, Cheng C, Sun H, Johnston J. Does diabetes target ganglion neurones? *Brain.* 2001; 124:2319–2334. [PubMed: 11673332]
56. Cheng C, Zochodne DW. Sensory neurons with activated caspase-3 survive long-term experimental diabetes. *Diabetes.* 2003; 52:2363–2371. [PubMed: 12941777]
57. Figueroa-Romero C, Iniguez-Lluhi JA, Stadler J, Chang CR, Arnoult D, Keller PJ, Hong Y, Blackstone C, Feldman EL. Sumoylation of the mitochondrial fission protein drp1 occurs at multiple nonconsensus sites within the b domain and is linked to its activity cycle. *FASEB J.* 2009; 23:3917–3927. [PubMed: 19638400]
58. Edwards JL, Quattrini A, Lentz SI, Figueroa-Romero C, Cerri F, Backus C, Hong Y, Feldman EL. Diabetes regulates mitochondrial biogenesis and fission in mouse neurons. *Diabetologia.* 2010; 53:160–169. [PubMed: 19847394]
59. Vincent AM, Edwards JL, McLean LL, Hong Y, Cerri F, Lopez I, Quattrini A, Feldman EL. Mitochondrial biogenesis and fission in axons in cell culture and animal models of diabetic neuropathy. *Acta Neuropathol.* 2010; 120:477–489. [PubMed: 20473509]

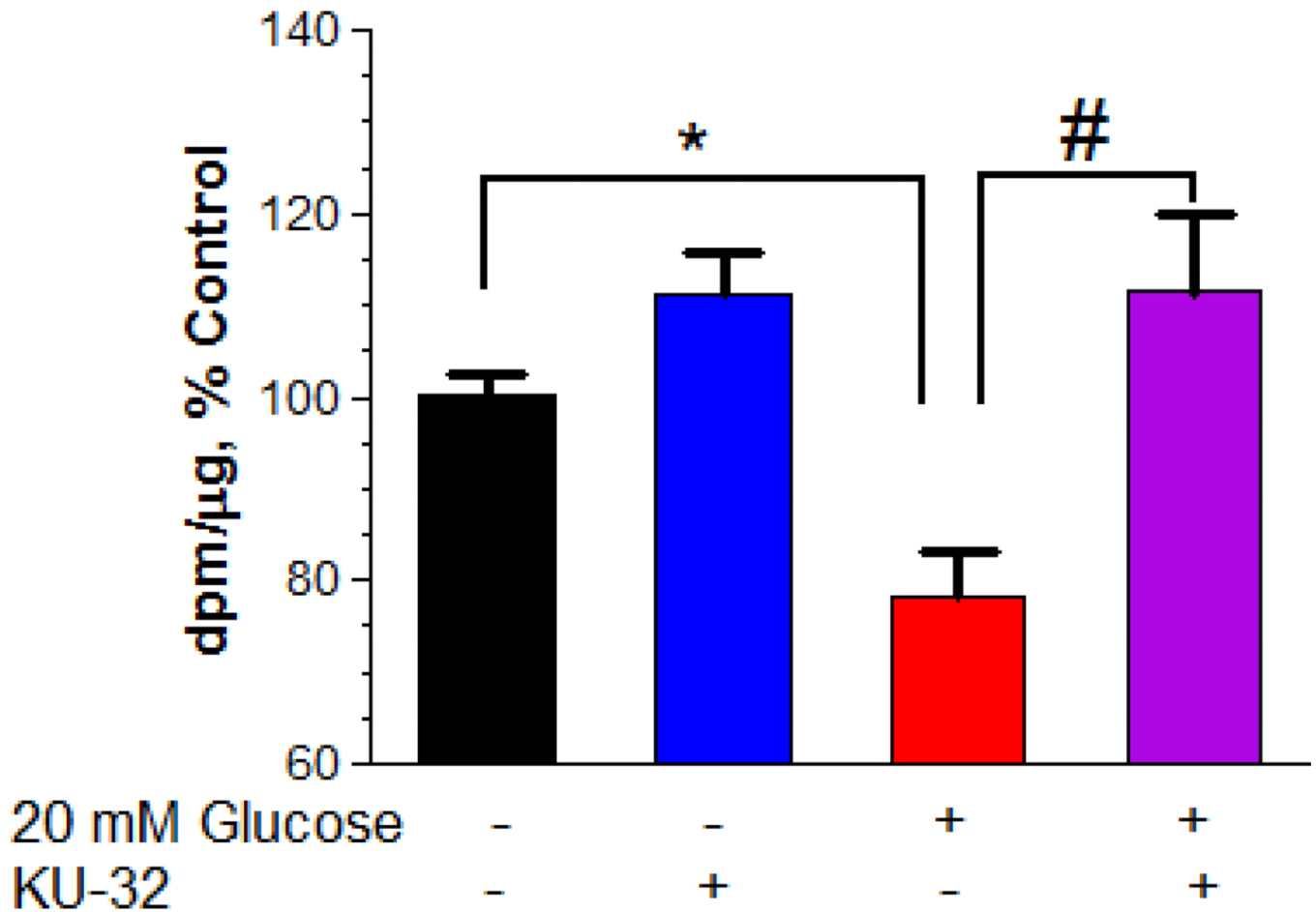


Figure 1. Hyperglycemia decreases the incorporation of [³H]Leucine into protein

Primary sensory neurons were cultured for 5 days in medium with 25 mM or 45 mM glucose and treated with DMSO or 1 μ M KU-32 for the final 24 hrs. Coincident with the addition of KU-32, the cells were pulsed with 1 μ Ci/ml [³H]Leu and the incorporation of [³H]Leu into total protein was determined as described in Experimental Procedures. The total dpm/ μ g protein was determined and the results are expressed as the percent of control. The data are the mean \pm SEM from three experiments. *, $p < 0.05$ compared to control, #, $p < 0.05$ compared to glucose minus KU-32.

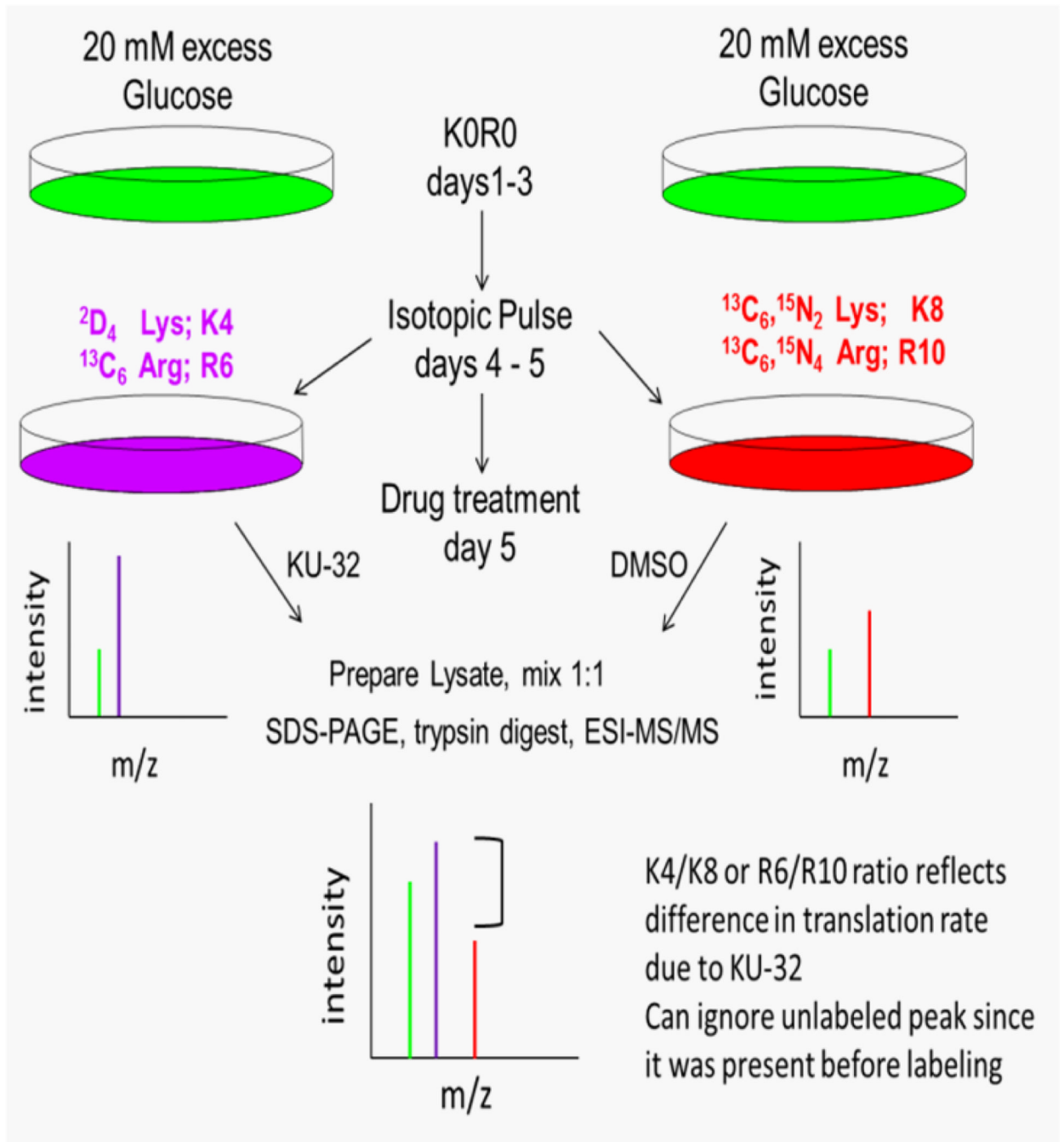


Figure 2. Experimental strategy for pSILAC analyses

Primary neurons were cultured in medium containing 45 mM glucose and light forms of Lys and Arg (KORO) for 3 days. The KORO cultures were divided in half and one set of cells was placed in hyperglycemic culture solution containing medium-heavy forms of Lys and Arg (K4R6). The cells were pulsed with K4R6 for 48 hrs and treated with 1 μM KU-32 for the final 24 hr. The remaining KORO cells were placed in hyperglycemic culture medium containing heavy isotope forms of Lys and Arg (K8R10) and treated with DMSO for the final 24 hr of the incubation. Total cell lysates were prepared, mixed in a 1:1 mass ratio, a heavy mitochondrial fraction isolated and the proteins separated by SDS-PAGE prior to tryptic digestion and MS/MS analysis.

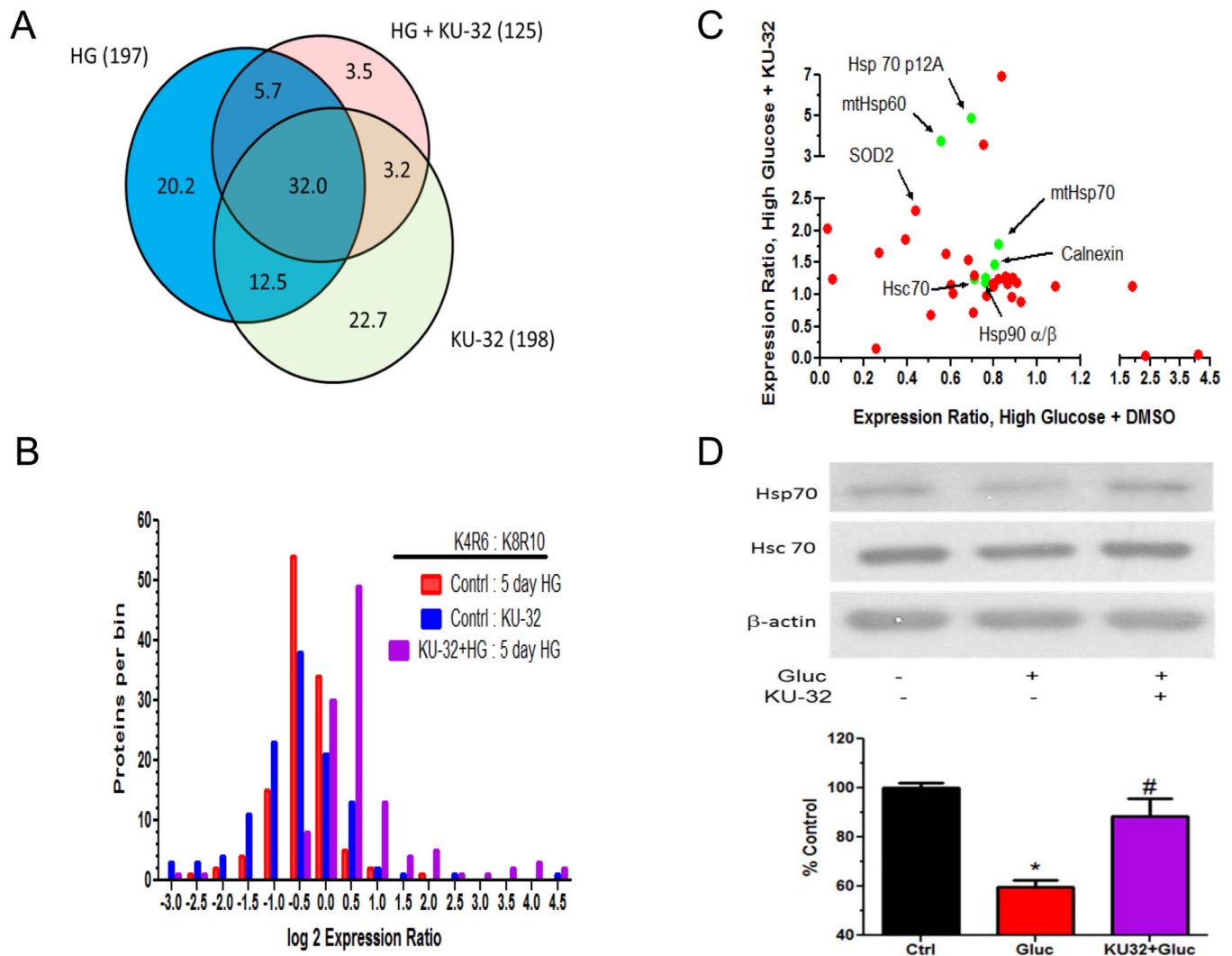
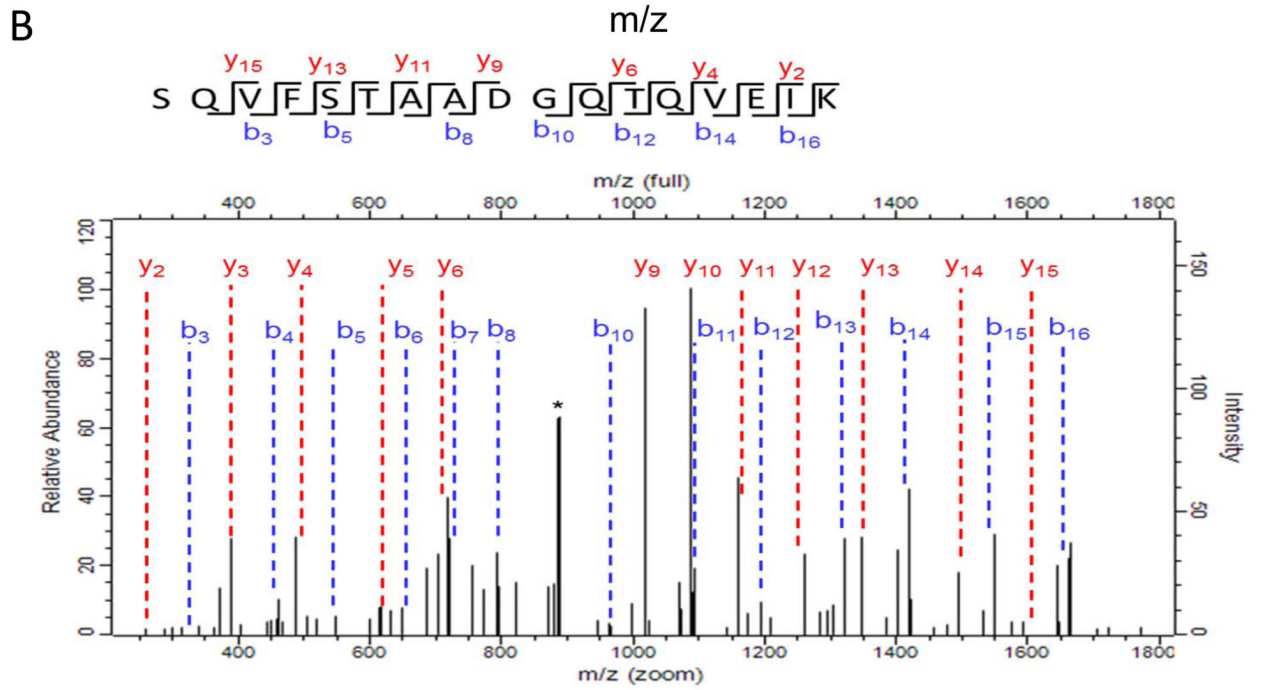
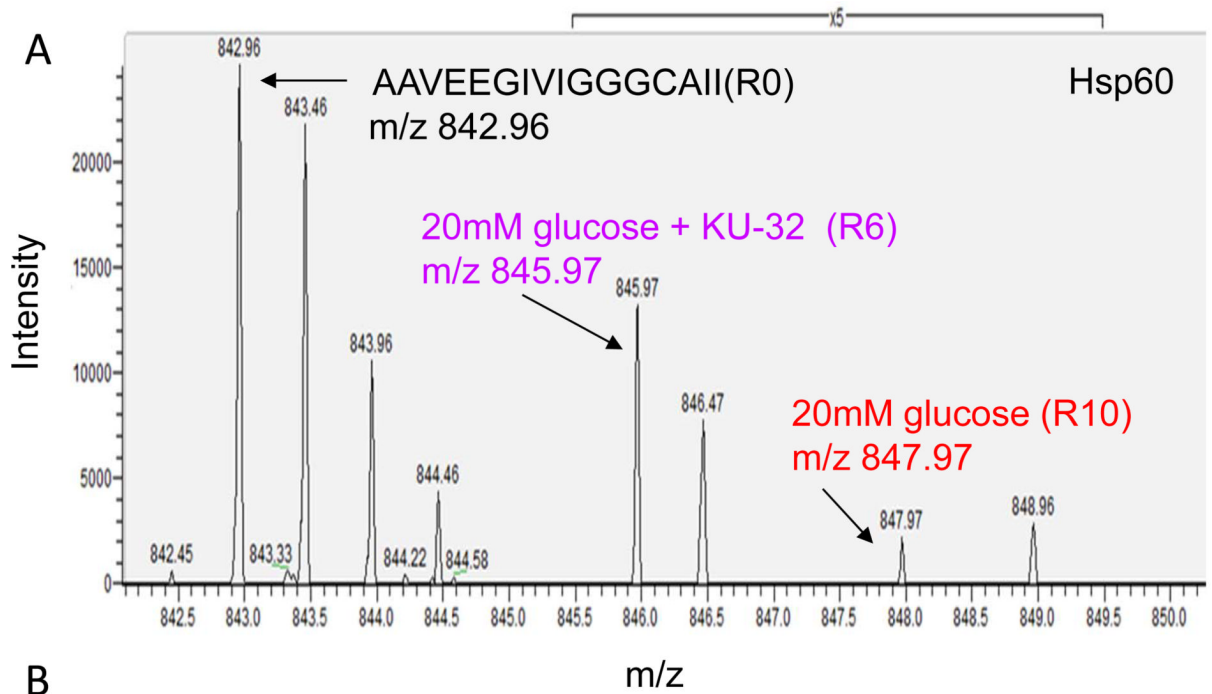


Figure 3. Distribution of translationally induced proteins

A) Venn diagram of quantified proteins in each group. Numbers in parentheses are total number of quantified proteins per treatment. Percent of unique and overlapping proteins are shown within the colored sections of the diagram. **B)** The non-normalized protein expression ratios provided by MaxQuant were log₂ transformed, binned into 0.5 units and the total proteins per bin counted. **C)** The expression ratios of all quantified chaperones (green) and mitochondrial proteins (red) detected in both the high glucose and high glucose + KU-32 treatments were plotted against each other. **D)** Representative immunoblot and quantitation of Hsp70 levels from three separate neuronal cultures. *, $p < 0.05$ compared to control, #, $p < 0.05$ compared to glucose minus KU-32.



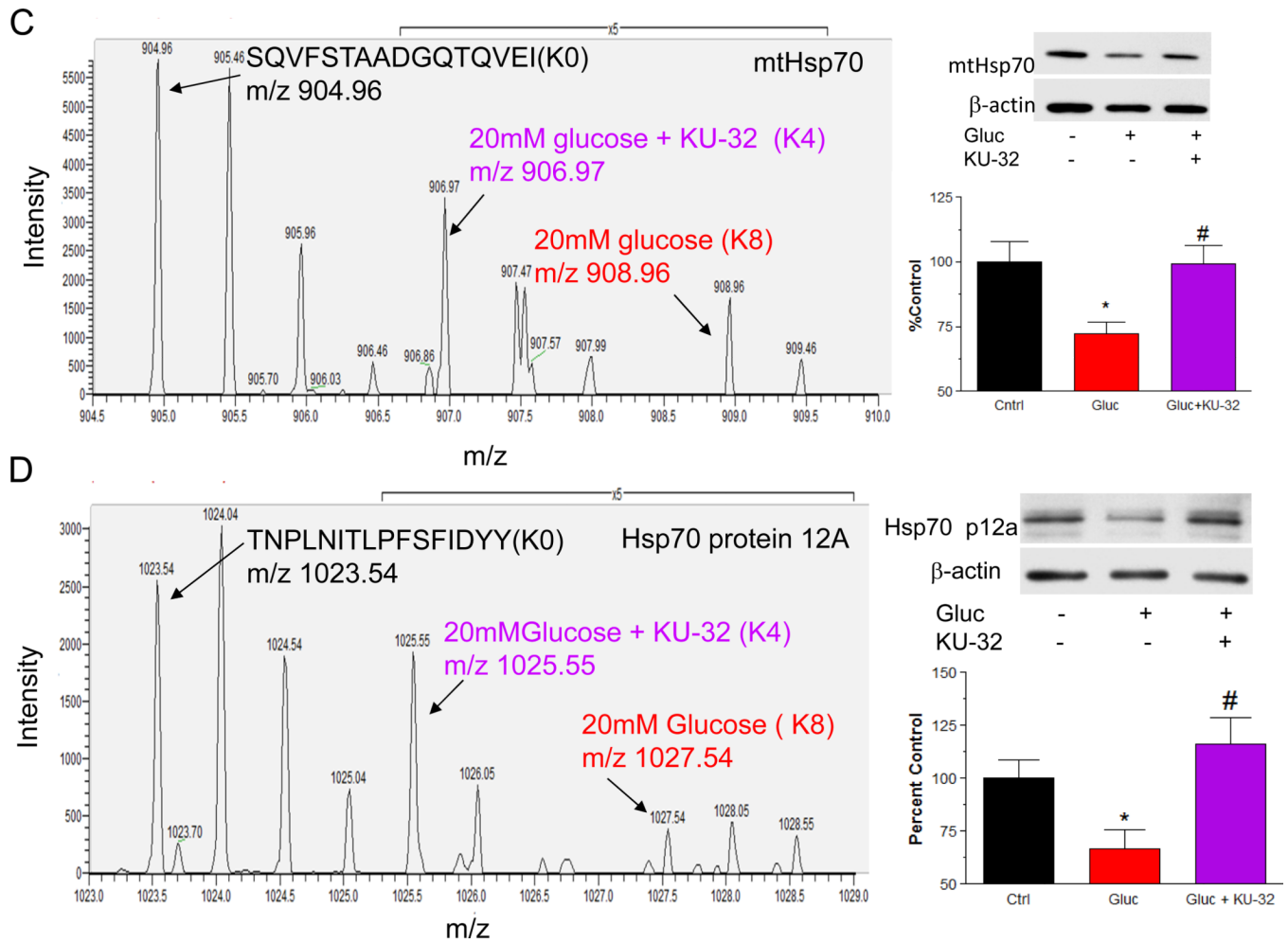
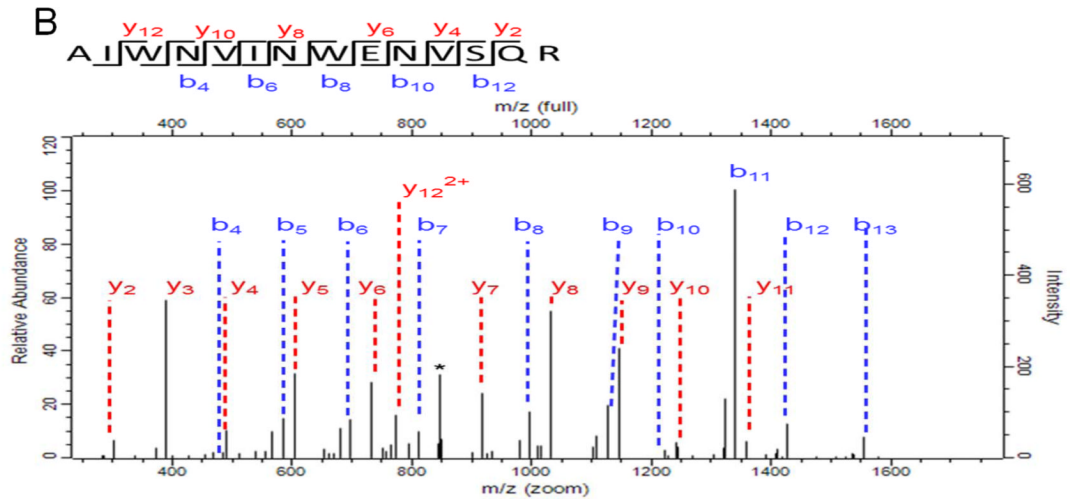
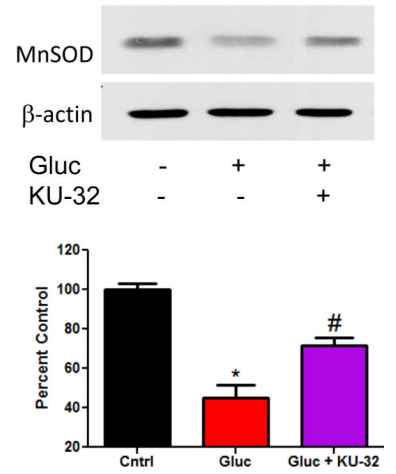
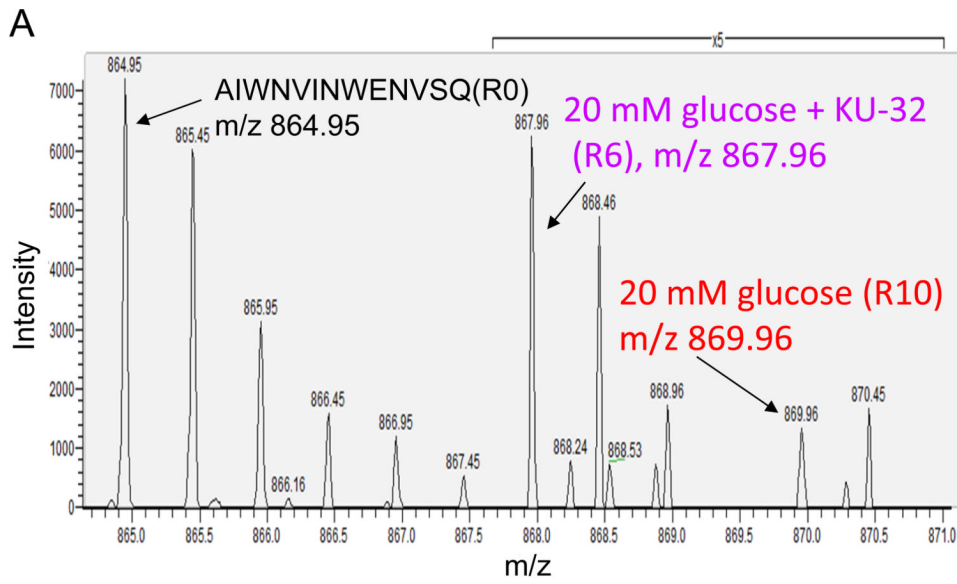


Figure 4. KU-32 induces the translation of Hsp60 and Hsp70 family members in hyperglycemic neurons

Primary neurons were incubated in medium containing 25 mM or 45 mM glucose for 3 days and pulsed with either K4R6 or K8R10 Lys/Arg for an additional 48 hrs. The cultures were treated with 1 μ M KU-32 (K4R6) or DMSO (K8R10) for the final 24 hrs of the incubation. Cell lysates were prepared, mixed in a 1:1 ratio and the samples processed for MS/MS analysis. (A) Representative MS scan showing an increase in Hsp60 in hyperglycemic neurons treated with KU-32 (R6 peptide) compared to glucose only (R10 peptide). Note the 5 \times scale amplification to demonstrate the increase in the R6 peptide compared to the R10 peptide. (B) MS/MS spectrum of the SQVFSTAADGQTQVEIK peptide of mtHsp70. The majority of the un-annotated peaks arise from the loss of water and ammonia ion but their labeling was omitted for clarity. The asterisk indicates a peak that was unassigned. (C) Representative MS scan showing an increase in mtHsp70 in hyperglycemic neurons treated with KU-32 (K4 peptide) compared to glucose only (K8 peptide); 5 \times scale amplification as discussed above. A representative immunoblot and quantitation (n=3) of the effect of hyperglycemia and KU-32 on mtHsp70 expression is shown to the right of the spectrum. (D) Representative MS scan showing an increase in Hsp70 p12A in hyperglycemic neurons treated with KU-32 (K4 peptide) compared to glucose only (K8 peptide); 5 \times scale amplification as discussed above. A representative immunoblot and quantitation (n=3) of the effect of hyperglycemia and KU-32 on Hsp70 p12A expression is shown to the right of the spectrum. *, p < 0.05 compared to control, #, p < 0.05 compared to glucose minus KU-32.



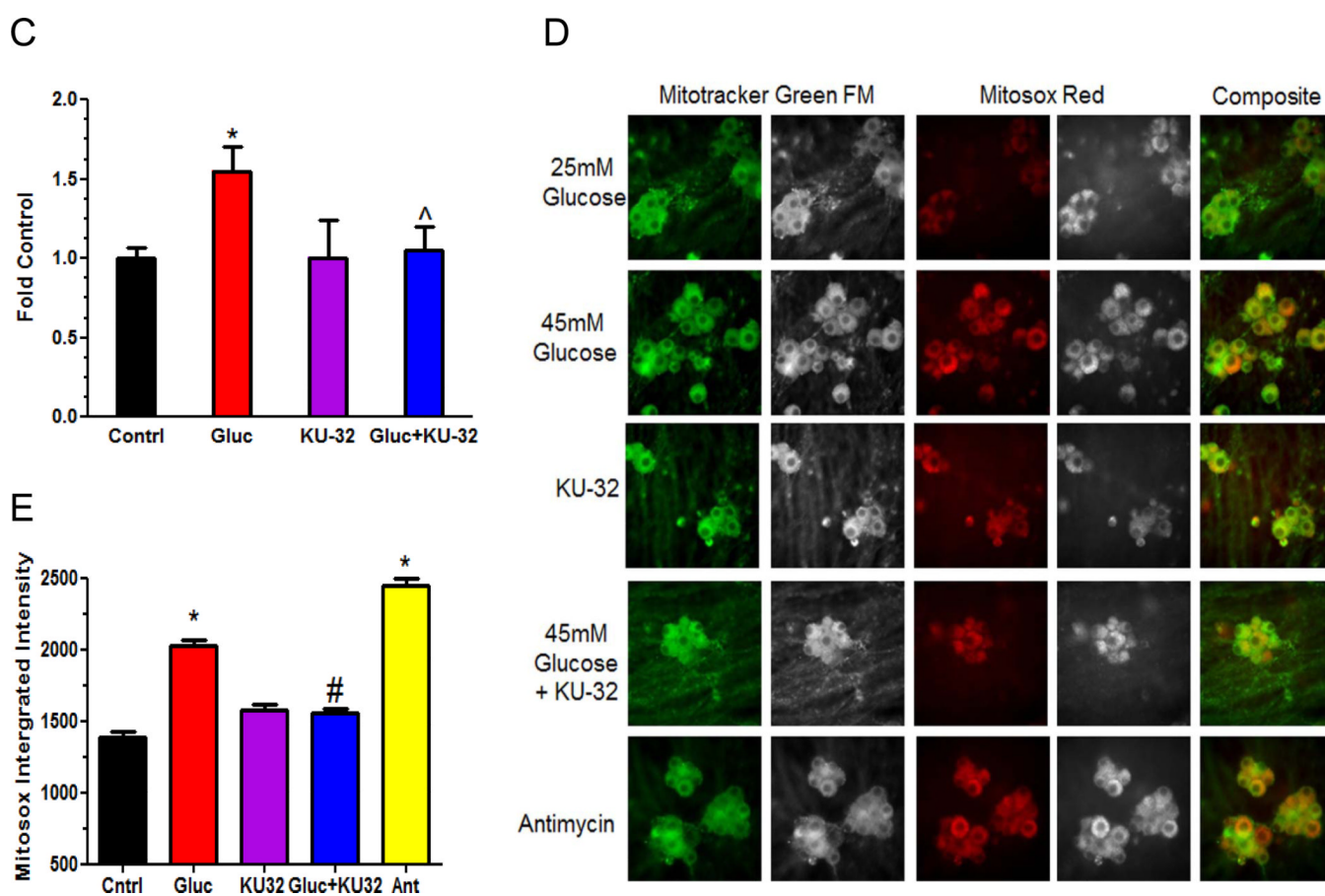


Figure 5. KU-32 induces the translation of MnSOD and decreases mitochondrial superoxide Hsp70 in hyperglycemic neurons

Primary neurons were incubated in medium containing 25 mM or 45 mM glucose for 3 days and pulsed with either K4R6 or K8R10 Lys/Arg for an additional 48 hrs. The cultures were treated with 1 μ M KU-32 (K4R6) or DMSO (K8R10) for the final 24 hrs of the incubation. Cell lysates were prepared, mixed in a 1:1 ratio and the samples processed for MS/MS analysis. (A) Representative MS scan showing an increase in MnSOD in hyperglycemic neurons treated with KU-32 (R6) compared to glucose only (R10). Note the 5 \times scale amplification to demonstrate the increase in the R6 relative to R10 peptide. A representative immunoblot and quantitation (n=3) of the effect of hyperglycemia and KU-32 on MnSOD expression is shown to the right of the spectrum. (B) MS/MS spectrum of the AIWNVINWENVSQR peptide. The majority of the un-annotated peaks arise from the loss of water and ammonia ion but their labeling were omitted for clarity. The asterisk indicates a peak that was unassigned. (C) Effect of KU-32 on decreasing glucose-induced superoxide production as measured using the ratio of ethidium/dihydroethidine. Results are expressed as a fold control and are the mean \pm SEM from three separate cultures. Gluc; 45 mM glucose. (D) Representative images showing that KU-32 decreased glucose-induced mitochondrial superoxide production as visualized using MitoSox Red. Neurons were co-stained with Mitotracker Green to localize mitochondria. Grey panels show raw grey scale images that were exported prior to being colorized in Image J. Cells treated with antimycin A (Ant) served as a positive control for superoxide generation. (E) Quantitative image analysis from three separate neuron cultures. *, p < 0.05 compared to control, #, p < 0.05 compared glucose minus KU-32.

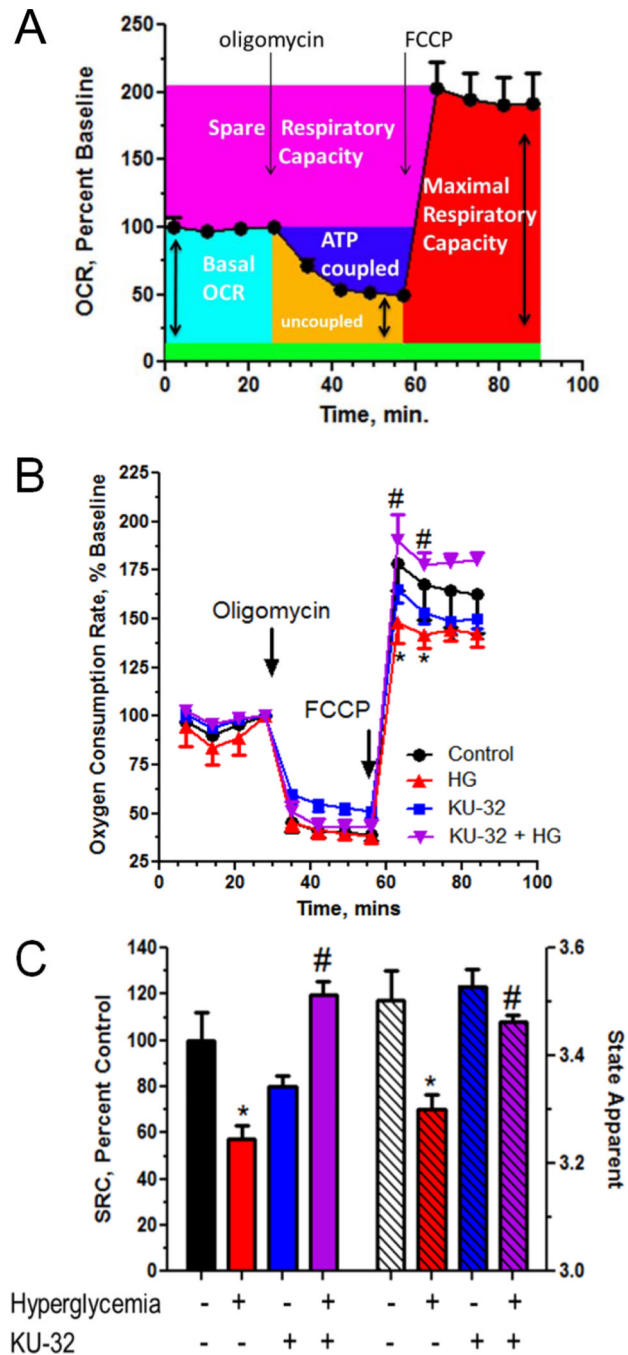


Figure 6. Hyperglycemia decreased mitochondrial bioenergetics which was reversed by KU-32 treatment

(A) Example of a mitochondrial function experiment in the XF96 extracellular flux analyzer. Basal OCR (light blue) is given by the first four rate measures. The addition of 1 $\mu\text{g/ml}$ oligomycin inhibits ATP synthase and the decrease in OCR gives a measure of ATP-coupled respiration (dark blue). Residual OCR in the presence of oligomycin provides a measure of proton leak (orange). The addition of 1 μM FCCP dissipates the proton gradient across the inner mitochondrial membrane and assesses maximal respiratory capacity (MRC, red). Spare respiratory capacity (SRC, pink) is assessed as the difference between MRC and the basal OCR. The green shading represents the estimated contribution of non-mitochondrial

respiration to basal OCR but was not directly measured in the experiment shown. **(B)** Primary neurons were seeded into a 96 well plate and incubated in medium containing 25 mM or 45 mM glucose for 5 days and treated with 1 μ M KU-32 or DMSO for the final 24 hrs. The cells were placed in medium containing 5 mM glucose and 1 mM pyruvate prior to the respiratory measures. Results shown are the mean \pm SEM from 5–8 wells per treatment from one experiment repeated three times. Arrows indicate the injection of oligomycin and FCCP. Hyperglycemia induced a significant decrease in MRC relative to control neurons (*, $p < 0.05$) and KU-32 treatment significantly increased MRC compared to cells treated with high glucose only (#, $p < 0.001$). **(C)** Hyperglycemia significantly decreased SRC (*, $p < 0.05$, left axis and solid bars) and State_{app} (*, $p < 0.01$, right axis and striped bars) compared to control cells. Both SRC (#, $p < 0.001$) and State_{app} (#, $p < 0.05$) were significantly improved by KU-32 treatment compared to cells treated with high glucose alone.

Table 1

Isotopic Combinations for pSILAC Experiments

Label Combination	Treatment	Ratio Analyzed	Interpretation
K4R6 (M) K8R10 (H)	25mM glucose 45mM glucose	H/M	Effect of 5 day hyperglycemia on translation
K4R6 (M) K8R10 (H)	25mM glucose 25mM glucose + KU-32	H/M	Effect of 24 hr KU-32 treatment on translation in basal glucose
K4R6 (M) K8R10 (H)	45mM glucose + KU-32 45mM glucose	M/H	Effect of 24 hr KU-32 treatment on translation under hyperglycemic conditions